High-Sensitivity Detection Method for Signals in PhyC-SN

Toshi Ito*, Osamu Takyu*, Mai Ohta‡, Takeo Fujii†, Koichi Adachi†
* Shinshu University, Nagano Japan, E-mail: takyu@shinshu-u.ac.jp
† The University of Electro-Communications, Tokyo Japan
‡ Fukuoka University, Fukuoka Japan

***Abstract*—There are two methods of collision detection in the wireless physical quantity conversion lump-sum collection method (PhyC-SN), in which sensor information is converted into carrier waves for transmission: energy detection alone and the use of features that utilize energy detection and frequency offsets together. The detection accuracy is better when features utilizing frequency offsets are used than when energy detection is used alone. However, the frequency offset causes a loss of orthogonality between subcarriers, resulting in inter-carrier interference, which degrades the accuracy of collision detection. In this paper, we propose a collision detection method that suppresses the effects of inter-carrier interference by applying a window function to the transmitted carrier wave with multiple symbols.**

I. Introduction

In recent years, sensor networks have become so widespread due to the development of communication technology that we are now in the IoT era[1]. The technology of simultaneous multiple connections has been attracting attention. In communication, it is necessary to communicate with many sensors quickly.

In the conventional packet communication method, when communicating with many sensors, the communication environment becomes congested, transmission efficiency decreases, and packets may be lost[2]. In addition, the communication cost becomes large because ID information is assigned to each packet. This paper focuses on a new communication method called PhyC-SN[3], which improves the transmission speed and reduces the transmission volume. Although it is still necessary to consider how to utilize PhyC-SN as a new communication method, a positioning method has been proposed as an example of utilizing PhyC-SN[4].

In certain situations, the PhyC-SN communication method has advantages over packet communication. However, PhyC-SN also has many problems. In this paper, as an initial study, we evaluate the effectiveness of high-sensitivity detection using window functions and support vector machines (SVM) for three patterns with 0, 1, and 2 or more sensors by simulating two features: energy value and phase variance utilizing frequency offsets.

II. Collision detection in PhyC-SN

A. PhyC-SN

The system model of PhyC-SN [5] is shown in Figure 1 . In Fig. 1, each sensor acquires temperature information and transmits the frequency corresponding to the temperature information. The receiver simultaneously receives the carrier wave sent from each sensor. The receiver processes the information according to the received frequency.

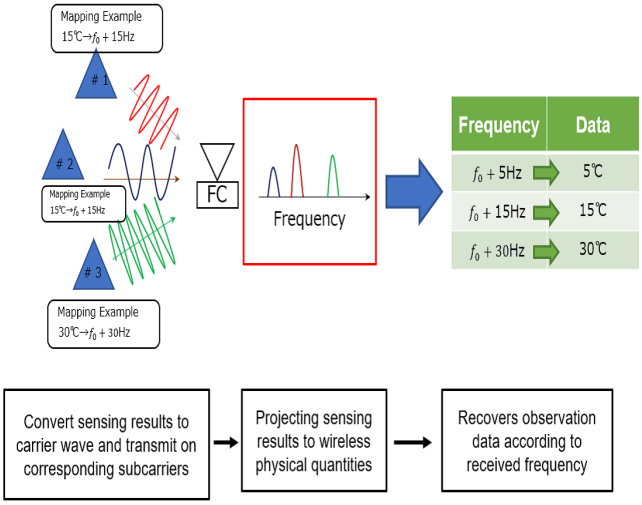

Fig. 1. PhyC-SN

B. Collision detection

In order to distinguish between one and two transmitting sensors on the same subcarrier, not only energy detection but also phase dispersion utilizing frequency offset has been used to improve the discrimination accuracy[6]. In this paper, we evaluate the identification accuracy of three patterns in which the number of sensors is 0, 1, or more than 2 at each subcarrier when multiple subcarriers are identified simultaneously using PhyC-SN.

C. Frequency Offset

Frequency offsets cause errors in the local carrier wave because the transmitter and receiver are not synchronized. Therefore, noise due to the frequency offset is introduced during reception, which causes inter-carrier interference. In this paper, we assume a low-cost product and a case where frequency offsets occur. The dispersion value of the phase transition amount that takes advantage of the phase transition amount caused by the frequency offset is used as a feature in the identification.

D. Variance value of phase transition amount

The following equation shows the variance value of the phase transition amount

$$\omega = \{(\hat{\theta}_1-\hat{\theta}_2)^2+(\hat{\theta}_1-\hat{\theta}_3)^2+\ldots+(\hat{\theta}_2-\hat{\theta}_3)^2+\ldots+(\hat{\theta}_{n-1}-\hat{\theta}_n)^2\} \quad (1)$$

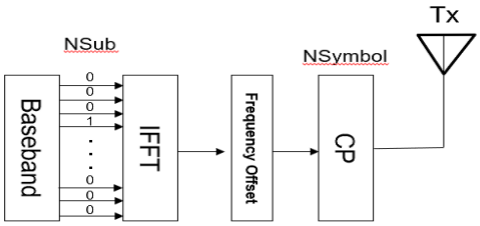

Fig. 2. Transmitter-side Processing

$$*\hat{\theta}_a - \hat{\theta}_b = \begin{cases} \hat{\theta}_a - \hat{\theta}_b & (\hat{\theta}_a - \hat{\theta}_b < 180) \\ 360 - \hat{\theta}_a - \hat{\theta}_b (\hat{\theta}_a - \hat{\theta}_b \geq 180) \end{cases}$$

$$\phi = \frac{\omega}{N(N-1)} \tag{2}$$

where θ_n denotes the phase transition at the nth receiving antenna, and a symbol is defined as a carrier wave divided by a certain time width, and the phase difference between two symbols is defined as the phase transition. In Eq. 1, the magnitude of the difference between each phase transition is calculated and expressed as the sum ω. Since the difference of the phase transitions is always the value with the smallest angular magnitude, if the difference of the phase transitions is greater than 180, the value of the difference of the phase transitions is subtracted from the total 360. In Eq. 2, the variance value of the phase transition ϕ is obtained by dividing ω by the number of antennas N and the number of antennas minus one, $N-1$.

III. High Sensitivity Detection

A. System Model

The system model transmitter and receiver in this paper is shown in Figure2 and Figure3. On the transmitter side, the actual data to be sent is set to 1 and the data not to be sent is set to 0. The data is IFFTed and then randomly frequency offset. This is done to represent the deviation of the carrier wave from the actual transmitter/receiver. Finally, the resulting carrier wave is used as one symbol, and the same symbol is duplicated and transmitted.

At the receiver side, noise is added immediately after receiving the transmitted carrier wave. The FFT is performed by applying a window function to this state over multiple symbols. This process increases the frequency resolution and produces a large number of frequency bin, so features are detected by synthesizing them for each subcarrier. Finally, SVM (Support Vector Machine) is used for restoration.

B. Window Function

Because of the frequency offset, inter-carrier interference must be considered. In some cases, window functions are used to suppress inter-carrier interference. For this reason, we are also evaluating the window functions when they are changed.

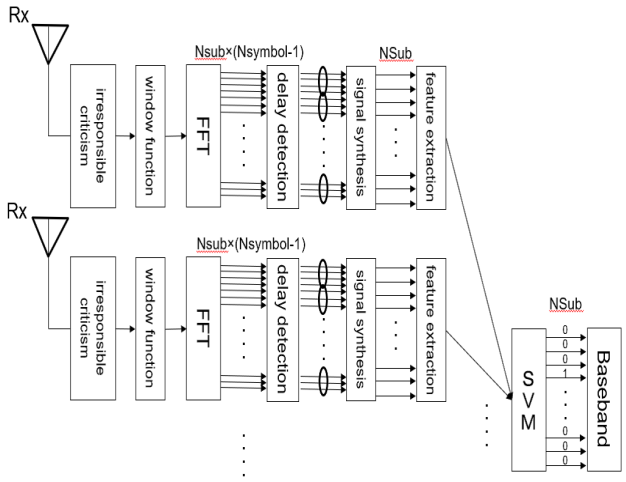

Fig. 3. Receiver-side Processing

There are various types of window functions, and the window functions employed in this study are rectangular windows and Blackman-Harris windows. Rectangular windows have a feature that the main lobe is sharp but side lobes are generated. The Black-Harris window has the feature that the main lobe is a little wider, but the sidelobes can be suppressed compared to other window functions. The Blackman-Harris window and the rectangular window are compared and evaluated.

Figure 4 is the FFT of multiple symbols multiplied by a rectangular window and a Blackman-Harris window. The vertical axis is the energy value and the horizontal axis is the frequency Bin. The spread of a transmission at a frequency Bin of 0 is shown. In the case of a rectangular window, the narrower the main lobe spread, the higher the energy value of the side lobes. In the Blackman-Harris window, the spread of the main lobe suppresses the energy values of the sidelobes. This is a trade-off relationship, and if the emphasis is on main lobe detection, the use of a rectangular window is more advantageous. Conversely, if the emphasis is on suppressing sidelobes, the use of a Blackman-Harris window is more advantageous.

C. Multiple Symbols

Since applying a window function to multiple symbols increases the FFT size, the window function is usually applied to a single symbol, as shown in the normal case of Fig.5. However, since the window function is combined with the first and the last symbols, the distortion caused by the window function becomes large when the window function is applied to a single symbol. Therefore, applying the window function to multiple symbols, as in the proposed method, suppresses the distortion caused by the window function and thus improves the detection accuracy. Moreover, by applying the window function to multiple symbols, the received frequency Bin for a single subcarrier can be viewed in detail. This fine view is

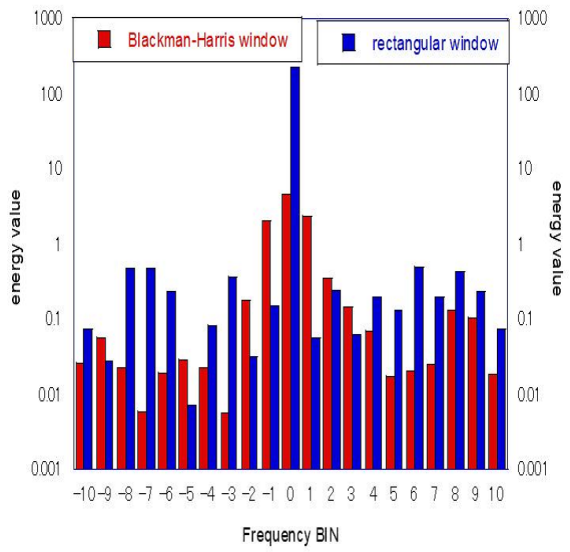

Fig. 4. Frequency Spread of Rectangular and Blackman-Harris windows

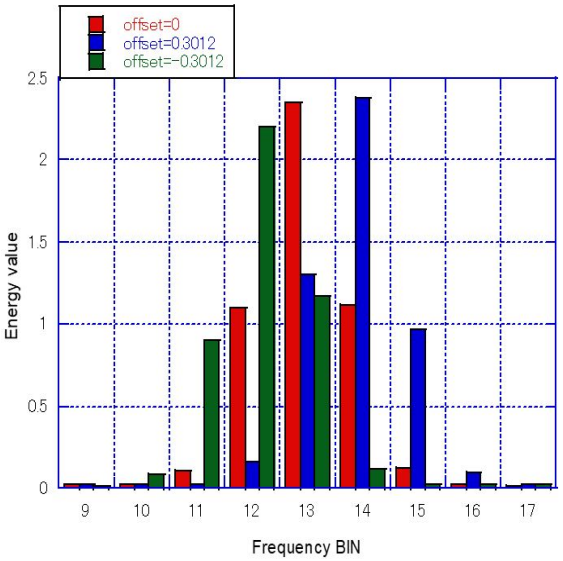

Fig. 6. Received frequency Bin example

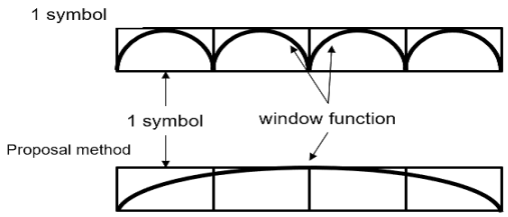

Fig. 5. Using Window Functions

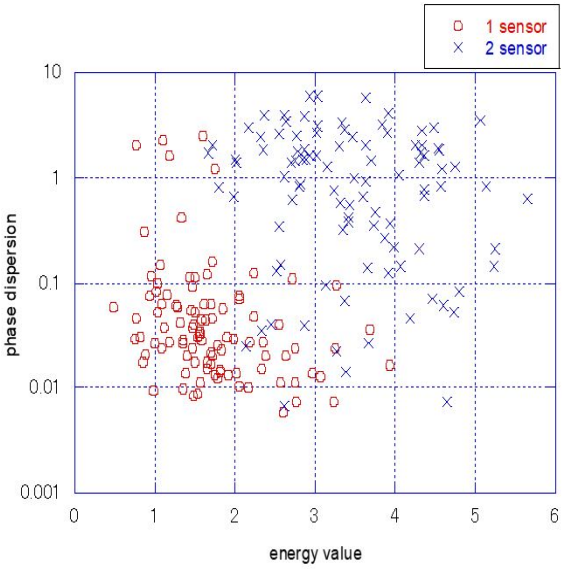

Fig. 7. Scatter Diagram

sensitive to the effect of frequency offset, which also affects the identification accuracy.

Figure 6 is an example of received frequency Bin. The vertical axis is the energy magnitude and the horizontal axis is the frequency Bin. Here, the frequency Bin corresponding to one subcarrier corresponds to 9 to 17. Each color represents the distribution of the energy value of one sensor during transmission, but with different frequency offsets applied to each. Red represents no frequency offset, blue and green are 0.3012 and -0.3012, respectively. By looking at the frequency Bin in detail, it can be seen that the peak points of the energy values due to the frequency offsets are different.

D. SVM (Support Vector Machine)

As a feature detection, Figure 7 is a scatter plot of energy values and phase variances for the cases when the number of sensors is one and two, respectively. The horizontal axis is the energy value and the vertical axis is the phase variance. In the conventional method, the energy value is used as the threshold value. In the areas with energy values of 2 and 3 in Figure 7, the number of transmitting sensors is 1 and 2, respectively, and it is difficult to distinguish them from each other. By adding the phase variance as a feature, it is possible to identify the number of transmitting sensors at energy values of 2 and 3. By determining the optimal boundary line for identifying the number of transmitting sensors (1 or 2), the accuracy of identification can be improved. SVM is used to create the optimal boundary. In this simulation, the SVM is parameterized and simulated by Matlab application, SVM that can be optimized by a classification learner.

Fig. 8. Experimental Environment

Sensor No.

data number	1	2	3	4	5	6	7	8	9	10	···	···	···	32	33	34	35
1	-54	-99	-103	-122	NaN	NaN	-88	-116	-118	-118	···	···	···	NaN	NaN	-125	NaN
2	-79	-108	-120	-125	-123	NaN	-83	-112	-122	-122	···	···	···	-115	NaN	NaN	NaN
3	-87	-113	-121	-120	NaN	NaN	-59	-108	-112	-122	···	···	···	-109	NaN	NaN	NaN

Fig. 9. Collected Data

IV. Simulation Overview

A. Experimental Data

In conducting this simulation, we used data from an actual case in which radio waves were emitted outdoors using 920 MHz band LoRa. As shown in Fig.8. The RSSI and the subcarriers were preliminarily matched with a quantization interval of 6 dB. The RSSI received by each sensor is recorded and transmitted from the sensor to the aggregation station on the frequency of the subcarrier corresponding to the RSSI.

Examples of collected data are shown in Figure 9. NaN is the value below the noise level, and in this experiment, the sensors do not transmit any signals to the aggregation station when the value is below the noise level.

Figure 10 shows the correspondence between the RSSI of data number 1 in Figure 9 and the subcarriers to be transmitted. The RSSI ranges from -136dB to -40dB and corresponds to subcarriers in 6dB intervals. . The number of transmitting sensors for each subcarrier is shown.

subcarrier number	1	2	3	4	5	6	7	8	9	10	11	12	13	14	15	16
RSSI value range	-136~ -130	-129~ -124	-123~ -118	-117~ -112	-111~ -106	-105~ -100	-99~ -94	-93~ -88	-87~ -82	-81~ -76	-75~ -70	-69~ -64	-63~ -58	-57~ -52	-51~ -46	-45~ -40
Data 1	0	2	4	3	1	1	1	1	0	0	0	0	0	1	0	0

Fig. 10. Correspondence chart between RSSI and Subcarriers

B. Simulation Evaluation

Using the experimental data, the number of sensors to be transmitted on each subcarrier is determined and the data is transmitted. The receiver processes the data and reconstructs it. The error rate of the restored data is evaluated. We compare five methods of restoration and evaluate their error rates. The second is an evaluation of the error rate when a rectangular window is applied to each symbol. The third is an evaluation of the error rate when a rectangular window is applied to multiple symbols. The fifth is the evaluation of the error rate when the Blackman-Harris window is applied to multiple symbols.

C. Error Rate

In this paper, we simulate the identification of three patterns in which the number of transmitting sensors is 0, 1, or 2 or more. The error rate in this simulation is the probability of misjudgment from the total, which is the value obtained by dividing the total by all the misjudgments such as when the number of transmitting sensors is 0 and the identification judgments are 1, 2 or more, or when the number of transmitting sensors is 1 and the identification judgments are 0, 2 or more.

TABLE I
Simulation Parameters

Data Type	usage data
Number of Receiving Antennas	10 antennas
Fading Environment	Rayleigh fading
Number of Subcarriers	16
Frequency Offset	random number per sensor of [-0.4 0.4]
Number of Window Symbols	9 Symbols
Window Function	Rectangular windows
	Blackman-Harris windows
Number of Sensors	35 sensors
Number of pre-training data	60 Data
Number of data for verification	64 Data
SNR	0,5,10,15,20[dB]

D. Simulation parameters

The simulation parameters are shown in Table I. In the Rayleigh fading environment, the number of receiving antennas is assumed to be 10. The number of subcarriers is 16. The frequency offsets are randomly assigned within the range of -0.4 to 0.4 of the normalized frequency spacing. Since this experiment assumes a low-priced product, the range of the magnitude of the frequency offset deviation is allowed to be wide. The window function is the Blackman-Harris window as

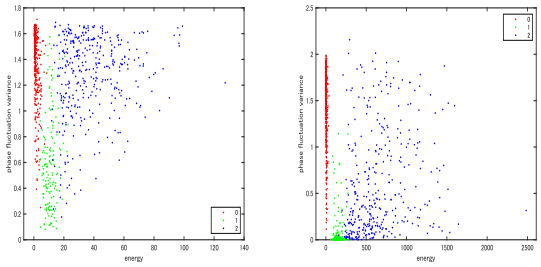

(a) Rectangular window(1 symbol)(b) Rectangular window(9 symbols)

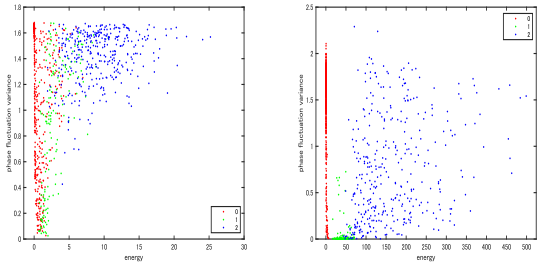

(c) Blackman-Harris window (1 symbol)

(d) Blackman-Harris window (9 symbols)

Fig. 11. Scatter Diagram

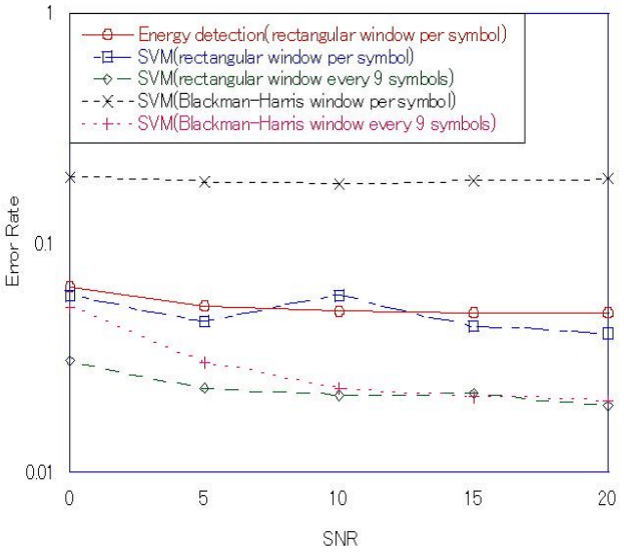

Fig. 12. Simulation Results

described above. The window function is applied to 9 symbols. The number of sensors is 35, and each sensor has 124 data. The error rates for 5 SNR values (0, 5, 10, 15, and 20 [dB]) are evaluated by simulation.

V. Simulation Results

A. Scatter Diagram

Figure 11 is a scatter plot of the window function multiplied by a rectangular window and a Blackman-Harris window with one symbol and nine symbols, respectively. The horizontal axis is the energy value and the vertical axis is the phase variance. When the window function is applied to each symbol, it is difficult to see the boundary line due to the difference in the number of sensors, but when the window function is applied to multiple symbols, the boundary line can be seen for each sensor algebra. However, when the window function is applied to multiple symbols, the boundary line becomes visible for each sensor algebra. When the window function is applied to multiple symbols, the phase dispersion for the number of transmitting sensors of 1 is suppressed. In Fig. 11(b) and Fig. 11(d), we can see that the phase variance is relatively lower in Fig. 11(d) when the number of sensors is 1.

B. Error Rate Evaluation

Figure 12 shows the simulation results. The vertical axis is the error rate and the horizontal axis is the SNR. In the case where a Blackman-Harris window is inserted for each symbol, the accuracy is worse than that of conventional energy detection due to the large effect of distortion caused by the window function. In other cases, the error rate was lower than that of energy detection by utilizing SVM. In addition, the use of multiple symbols reduces the distortion caused by the window function, resulting in a lower error rate. In terms of rectangular windows, applying rectangular windows to multiple symbols, rather than rectangular windows to each symbol, allows us to see the effects of frequency offsets in detail, and the difference in the number of features depending on the number of sensors reduces the error rate.

VI. Summary

High-sensitivity detection was performed to improve the identification accuracy of sensors with 0, 1, and 2 or more sensors using the physical quantity conversion batch collection method (PhyC-SN). The window function was changed to suppress inter-carrier interference. When the window function was applied to each symbol, the identification accuracy was degraded due to the distortion caused by the Blackman-Harris window. On the other hand, when the Blackman-Harris window was applied to multiple symbols, the distortion caused by the window function was suppressed, leading to a reduction in the error rate. Also for rectangular windows, changes were observed depending on the number of symbols over which the window function was applied. Frequency resolution can be increased by applying the window function to multiple symbols. Therefore, since the effect of frequency offset can be observed more precisely, even for the rectangular window, applying the window function to multiple symbols increased the difference in the feature values depending on the number of sensors, leading to a decrease in the error rate. Comparing the window functions, the rectangular window leads to a lower error rate than the Blackman-Harris window in this study.

VII. Future

As an initial study, we have evaluated the discrimination accuracy for the number of sensors above 0, 1, and 2, and are considering increasing the number of sensors that can be discriminated. By increasing the frequency resolution, we are able to perform detailed analysis. We would like to focus on the frequency spread as a new feature to be considered in the future.

Acknowledgement

A part of this research project is sponsored by the Ministry of Internal Affairs and Communications in Japan under the Strategic Information and Communications R & D Promotion Programme (SCOPE JP205004001) and JSPS KAKENHI Grant Number JP21H01322.

References

[1] J. M. Williams et al., "Weaving the Wireless Web: Toward a Low-Power, Dense Wireless Sensor Network for the Industrial IoT," in IEEE Microwave Magazine, vol. 18, no. 7, pp. 40-63, Nov.-Dec. 2017.

[2] J. Sa-Ingthong, A. Phonphoem, A. Jansang and C. Jaikaeo, "Probabilistic Analysis of Packet Losses in Dense LoRa Networks," 2021 13th International Conference on Knowledge and Smart Technology (KST), Bangsaen, Chonburi, Thailand, 2021, pp. 225-230.

[3] O. Takyu, K. Shirai, T. Fujii and M. Ohta, "Adaptive Channel Assignment With Predictions of Sensor Results and Channel Occupancy Ratio in PhyC-SN," in IEEE Access, vol. 7, pp. 44645-44658, 2019.

[4] M. Oda and O. Takyu,"Position Estimation with Radio Sensor in Physical Wireless Parameter Conversion Sensor Networks",IEICE 2021 International Conference on Emerging Technologies for Communications (ICETC 2021),pp. 1-4 (online) (December 3, 2021).

[5] Fujii et al, "Highly efficient collection of multiple sensor information - Utilization of information exchange to wireless geophysical quantities -," Shinagawa Giho, Japan. CCS2012-036, March 2012.

[6] T. Ito, O. Taku, K. Adachi, M. Ota, and T. Fujii, "Collision Detection with Frequency Offset and Energy Detection in the Physical Quantity Transformation Batch Collection Method," General Conference, March 2022.